

Removing Streak Interference from a Single Image based on Joint Priors

Ao Li^a, Xin Liu^a, Deyun Chen^a, Kezheng Lin^a, Guanglu Sun^a, and Qidi Wu^{b,*}

^a*School of Computer Science and Technology, Harbin University of Science and Technology, Harbin, 150080, China*

^b*College of Information and Communication Engineering, Harbin Engineering University, Harbin, 150001, China*

Abstract

Streaks due to weather, such as rain or snow, degrade image quality and affect the performance of subsequential high-level vision tasks by the generated undesired artifacts. Hence, removing streak interference is an ongoing and challenging issue for many applications in real-time mobile surveillance systems. In this paper, streak interference removal from a single image is the focus. To sufficiently extract streak interference from an observed image, the image was firstly filtered with the nonsubsampling contourlet transform. Then, the residual part between the original and filtered image was decomposed into the streak component and detail component of background. Based on the additive layer model, we designed two specific priors that constrain the detail and streak interference respectively and established a model with joint priors for residual image decomposition. As a result, the resulting image can be synthesized with the filtered image and detail component. Experimental results show that our proposed method outperforms existing methods both qualitatively and quantitatively.

Keywords: removing streak interference; nonsubsampling contourlet transform; sparse representation; Gaussian mixture model; prior

(Submitted on August 17, 2018; Revised on September 5, 2018; Accepted on October 23, 2018)

© 2018 Totem Publisher, Inc. All rights reserved.

1. Introduction

In the era of big data, millions of outdoor surveillance systems are placed everywhere throughout our city, and they are significant video collection devices in modern life. With these surveillance systems, billions of images are produced every day, which can be used to help to improve traffic controlling and public security. Nevertheless, it is inevitable that the images are affected by some weather conditions, such as rain or snow. Therefore, some undesired streak interference will be presented to degrade the visual quality and produce extra influence on subsequential tasks, such as recognition, object detection [1-2], and image analysis [3]. Some analyses on the interference from the view of fractal math have been proposed to facilitate improvement [4-6]. Hence, the streak interference removal has attracted much attention and is widely studied in recent years.

To our best knowledge, streak interference removal can be categorized into two main kinds based on the type of input data. The first kind involves video-based streak removal approaches. Through a comprehensive analysis on the visual effect of rain in imaging systems, Garg et al. proposed a rain removal method with two creative visual models [7]. They firstly designed a correlation model to capture the dynamics for rain streaks. Then, a physical-based motion model was developed, which is used to explain the photometry of rain. In [8], incorporating temporal and chromatic information, a rain removal algorithm was proposed for both the stationary and dynamic scenes taken from a stationary camera. In this method, the temporal information was used to state that rain could not always cover the same pixels throughout the entire video, and the chromatic property told us that the change of values is approximately the same in the three channels of RGB space. Next, Barnum et al. [9] thought that dynamic weather interference has a predictable global effect in the frequency domain, so a model for shaping the appearance of a single raindrop or snow streak in the spatial space was developed. Then, it was combined with the statistic characteristics of streak to generate another model of the overall effect of weather interference in the frequency domain. This model can be used to detect the streak firstly, and the weather interference can be removed with the detection results. To better separate the streak of rain or snow from the background of sequences, [10] proposed the photometry-based selection rules that were used to select the potential streak interference. Then, the histogram of

* Corresponding author.

E-mail address: iseeklin@163.com

orientations of streaks, which was assumed to follow the Gaussian uniform mixture model, is calculated to help remove the weather interference due to the different distributions of streak and noise. Nevertheless, it is noted that, benefiting from the sufficient spatial-temporal information, the aforementioned methods can achieve good performance in removing the streaks as fast variational components in video. The other category is the streak removal from a single image, which is a more challenging problem due to its limited scene information. Kang et al. firstly proposed an effective framework, which took the rain removal as an image decomposition problem. In [11], the decomposition is implemented via morphological component analysis (MCA). Different from the conventional MCA-based decomposition, the rain component is removed from the high-frequency part of the observed image, which avoids the interference of complicated backgrounds and extracts purer rain components. Similarly, an extended method based on decomposition is proposed in [12], where the image was divided into different groups, and the context-constraint segmentation and group-specific dictionaries were learned to better recognized the background and rain patterns. To improve the representation performance, a discriminative dictionary was learned in [13] to separate the rain layer upon a nonlinear generative model, which demonstrates an advantage on visual effects of rain removal. From the viewpoint based on regularization, Chen et al. [14] proposed a generalized low rank model in order to characterize spatial-temporal rain streaks, which extended the conventional prior model from matrix to tensor structure. The obtained promising results verified the effectiveness of their proposed method. To better characterize the layer in images, Li et al. [15] proposed to take different Gaussian mixture models as the priors to constrain the background and rain layers respectively, which was believed to help capture the multiple orientations of complex rain streaks.

In this paper, we addressed the problem of streak interference removal from a single image. Motivated by the aforementioned works, we proposed to establish a comprehensive optimization model for streak removal based on joint priors. Firstly, instead of implementing removal on the original, we filtered the image with nonsubsampling contourlet transform to separate the streak interference sufficiently. Next, two layer-based priors were individually designed to constrain the details of background and streak interference, and an objective function for the removal model was proposed with these two joint priors to obtain the streak interference layer. Finally, the desired streak removal image was synthesized with the pure details of the background and filtered image.

The rest of the paper is organized as follows. Section 2 presents the details of our proposed method, including the designed priors and comprehensive framework. Section 3 develops a numerical scheme for the objective function in the proposed framework. Several experimental results on test data are presented in Section 4. Section 5 summarizes the paper.

2. Our Streak Interference Removal Model

2.1. Image Filtering with Nonsubsampling Contourlet Transform

A key problem in our proposed framework is how to model the layer of the background and streak interference respectively. Due to the redundant background information in outdoor nature images, it is difficult to find the separable and suitable priors to directly characterize the different layers in images. Moreover, pure streak interference extraction plays an important role in capturing the streak patterns, which was firstly detected with the temporal information in video-based removal methods. However, in a single image, no sufficient temporal background information can be utilized, resulting in the streak removal being more challenging. In addition, due to the large mixture of complicated backgrounds and streak interference, it is not easy task to separate them. Hence, similar to the idea presented in [11], the image must be roughly separated into two parts: the basic background part and the streak interference part with contour details. Suppose that an observed image I can be modeled as follows.

$$I = I_B + I_{SC} \quad (1)$$

Where I_B denotes the coarse background image and I_{SC} denotes the streak interference image with contour details.

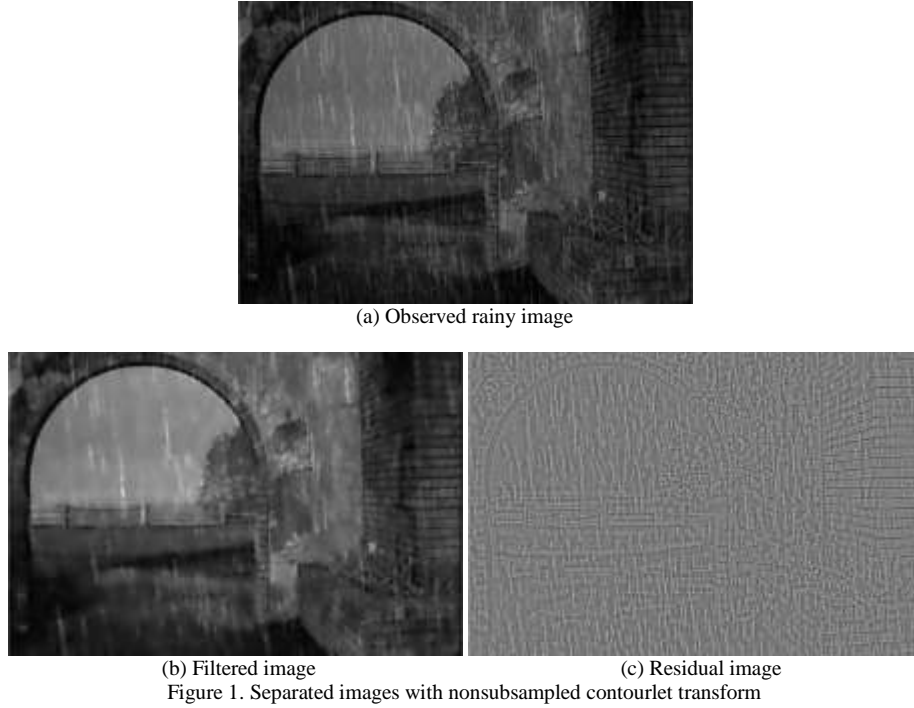
Recently, the multi-scale analysis tools (MSAT) were proposed and are widely used in many applications of image problems, such as restoration [16] and fusion [17]. It is noted that MSAT have a powerful ability to decompose images in terms of frequency division and capture the texture details. In our method, the nonsubsampling contourlet transform [18], which has favorable scale-preserving property, is used to separate the observed image I into I_B and I_{SC} . Assuming that $T_{NSCT}(\bullet)$ denotes the nonsubsampling contourlet filtering operator, the background I_B can be obtained by the following formulation.

$$\hat{I}_B = T_{NSCT}(I) \quad (2)$$

Next, the I_{SC} can be computed as the residential component between the observer image and the coarse background with

$$I_{SC} = I - T_{NSCT}(I) \quad (3)$$

Figure 1 shows the separation results of our filtered method, from which we can obviously see that the streak interference with parts of detailed textures are explicitly separated. The results are helpful to extract the pure geometric details and streak interference.



2.2. Proposed Objective Function

In this section, we will discuss how to establish an effective objective function that can decompose the image into geometric and streak interference components. In our framework, instead of implementing the decomposition to the observed image directly, we will decompose the residual image I_{SC} to alleviate the influence of the complicated background scene. That is, due to the compact contour information and massive streak interference included in the I_{SC} , it is easier to extract the streak layer and geometric component accurately. Assuming that I_{SC} is synthesized with the following layer-based model,

$$I_{SC} = S + G \quad (4)$$

Where S and G denote the streak interference component and geometric details component respectively.

With the formulation in (4), what we desire is to construct a suitable decomposition method that can separate the two latent components sufficiently. To this end, by the maximum posterior in Bayesian theory, the following objective function is proposed to implement the decomposition.

$$\min_{S,G} \left(\|I_{SC} - S - G\|_F^2 + \Omega(S) + \Psi(G) \right) \quad (5)$$

Where $\|\bullet\|_F$ denotes the Frobenius norm to control the fidelity between the residual image and its decomposed components. The second and third terms are used to constrain some joint priors on streak interference and geometric details. It is noted that the form of the joint priors plays a significant role in the performance of streak removal. Next, we will focus on the construction of these two priors to obtain a better decomposition result.

As for the geometric details component, a sparse representation-based prior is designed as follows.

$$\Omega(S) = \sum_i \left(\|v(S_i) - D_s \alpha_i\|_2^2 + \eta \|\alpha_i\|_1 \right) \quad (6)$$

Where $v(\bullet)$ denotes a vectorized operator, S_i presents a patch centralized around i^{th} pixel of S , D_s denotes the local dictionary to sparsely represent the patches, α_i denotes the sparse coefficient for i^{th} patch, and η is a positive scalar to balance the two terms. Considering the complicated textures of the geometric details component, we utilize the sparsity prior to constrain its patches. Also, it is worth noticing that the geometric details have more abundant structures than the streak interference, whose local orientations are nearly consistent in the whole image. Thus, to capture more details, a local dictionary D_s is pre-learned, by KSVD [19], from massive non-rainy training images.

Though a similar sparsity constraint can be forced on the streak interference layer, there are two main drawbacks that will limit the performance. First, we cannot obtain enough training samples for streak interference as the general natural image. Nevertheless, the sufficient samples have a great influence on the dictionary performance. Second, due to the different patterns of streak in different images, it is a good choice to train a better prior from the observed image itself. The Gaussian mixture model (*GMM*) is a recent popular prior and extensively used in many image inverse problems [20]. In [20], *GMM* has been verified to be a better learning-based prior and is advantageous in the patch-based method to obtain a high quality whole image. Based on this discussion, the following prior for streak interference is defined as:

$$\Psi(G) = -\lambda \sum_i \ln(GMM(v(G_i))) + \tau \|G\|_F^2 \quad (7)$$

Where λ and τ are two positive scalars to balance the two terms. $GMM(\bullet)$ stands for the Gaussian mixture function.

$$GMM(x) = \sum_{k=1}^N \pi_k N(x | \mu_k, \Sigma_k)$$

Where $N(\bullet)$ stands for the Gaussian distribution, μ_k and Σ_k respectively denote the mean and covariance matrix for the k^{th} Gaussian component, and π_k denotes the weight such that $\sum_{k=1}^N \pi_k = 1$. The first term in Equation (7) is the expected patch-based log likelihood to model the streak interference. The second term is the power constraint versus the large oscillation controlled by the image bound.

Substituting Equations (6) and (7) into Equation (5), we can obtain the proposed objective function for decomposition model as follows.

$$\min_{S, G} \left(\|I_{SC} - S - G\|_F^2 + \sum_i \left(\|v(S_i) - D_s \alpha_i\|_2^2 + \eta \|\alpha_i\|_1 \right) + \tau \|G\|_F^2 - \lambda \sum_i \ln(GMM(v(G_i))) \right) \quad (8)$$

With the approximation such that $v(S_i) \approx D_s \alpha_i$, Equation (8) can be rewritten as the following more compact form.

$$\min_{\alpha, G} \left(\|I_{SC} - D_s \circ \alpha - G\|_F^2 + \eta \|\alpha\|_1 + \tau \|G\|_F^2 - \lambda \sum_i \ln(GMM(v(G_i))) \right) \quad (9)$$

Where

$$S \approx D_s \circ \alpha = (\sum_i R_i^T R_i)^{-1} (\sum_i R_i^T D_s \alpha_i)$$

R_i is the operator to extract $v(S_i)$ from S , and $\eta\|\alpha\|_1 \approx \sum_i \eta\|\alpha_i\|_1$. In Equation (9), the local dictionary, which was learned from various training images, is used to represent the abundant textures existing in the geometric details of the background. Meanwhile, the GMM prior, which has distinguished ability to characterize the patterns of patches, is forced on the streak interference component to obtain a purer streak layer.

3. Solution Scheme for Objective Function

In this section, a numerical solution scheme is developed to solve the proposed objective function in Equation (9). As noticed in Equation (9), it is non-convex with the two variables. Therefore, some splitting techniques could be exploited to obtain the approximate optimal solution alternatively. To this end, an auxiliary variable p_i is firstly introduced, and Equation (9) can be rewritten as follows.

$$\min_{\alpha, G} \left(\|I_{SC} - D_S \circ \alpha - G\|_F^2 + \eta\|\alpha\|_1 + \tau\|G\|_F^2 - \lambda \sum_i \ln(GMM(p_i)) \right) \quad (10)$$

$$s.t. \quad p_i = v(G_i), \forall i$$

Then, transform Equation (10) to the unconstraint form as:

$$(\hat{\alpha}, \hat{G}, \hat{p}_i) = \arg \min \left(\|I_{SC} - D_S \circ \alpha - G\|_F^2 + \eta\|\alpha\|_1 + \tau\|G\|_F^2 + \gamma \sum_i \|p_i - v(G_i)\|_2^2 - \lambda \sum_i \ln(GMM(p_i)) \right) \quad (11)$$

Where γ is a regularization parameter increasing during the iteration, which will make the solution closer to that of Equation (9). The detailed iterative scheme is presented as follows.

In the n^{th} iteration, with a fixed $G^{(n)}$ and $p_i^{(n)}$, the sub-problem for $\alpha^{(n+1)}$ can be obtained as:

$$\alpha^{(n+1)} = \arg \min \left(\|I_{SC} - D_S \circ \alpha - G^{(n)}\|_F^2 + \eta\|\alpha\|_1 \right) \quad (12)$$

With the definition in Equation (9), the problem in (12) can be approximately solved in the following patch-wise way.

$$\forall i, \alpha_i^{(n+1)} = \arg \min \left(\|v((I_{SC})_i - G_i^{(n)}) - D_S \alpha_i\|_2^2 + \eta\|\alpha_i\|_1 \right) \quad (13)$$

Note that Equation (13) is a standard l_1 -norm based sparse coding problem, and each $\alpha_i^{(n+1)}$ can be computed with the pursuit algorithm in [21].

Similarly, given $\alpha^{(n+1)}$ and $p_i^{(n)}$, the sub-problem for $G^{(n+1)}$ is expressed as:

$$G^{(n+1)} = \arg \min \left(\|I_{SC} - D_S \circ \alpha^{(n+1)} - G\|_F^2 + \tau\|G\|_F^2 + \gamma \sum_i \|p_i^{(n)} - v(G_i)\|_2^2 \right) \quad (14)$$

This is a quadratic problem, and the closed-form solution can be computed by the following formulation.

$$G^{(n+1)} = \rho(I_{SC} - D_S \circ \alpha^{(n+1)} + \Theta) \quad (15)$$

Where ρ is a scalar such that $\rho = \frac{1}{\gamma + \tau + 1}$, and Θ presents the aggregation image such that $\Theta = \left(\sum_i R_i^T R_i \right)^{-1} \left(\sum_i R_i^T p_i^{(n)} \right)$.

By fixing $G^{(n+1)}$ and $\alpha^{(n+1)}$, the sub-problem associated with p_i is separable for each patch and can be formulated as:

$$p_i = \arg \min \left\{ \left\| p_i - v \left(G_i^{(n+1)} \right) \right\|_2^2 + \ln \left(GMM \left(p_i \right) \right) \right\} \quad (16)$$

For the objective function in (16), an approach, which implemented the Wiener filtering to the Gaussian component with largest weight, is suggested in [20] to obtain its approximate solution and guarantee the convergence. To train a more effective *GMM* for representing the pattern of streak interference, as suggested in [15], we can select some smooth area in the image to extract the training samples. It can make the patches more approachable to the pure streak component.

With the discussion, the overall scheme is summarized as follows.

Table 1. Solution scheme
Solution scheme for Equation (10)
Initial: Residual image I_{sc} , Learned dictionary D_s , GMM, and maximum iteration number N ;
while $n < N$
1. For $\forall i$, computed $\alpha_i^{(n+1)}$ with Equation (13);
2. Computed $G^{(n+1)}$ with Equation (15);
3. For $\forall i$, computed $p_i^{(n+1)}$ with Equation (16);
4. $n \leftarrow n+1$;
end while

By the decomposition result of the scheme, the geometric detail component can be computed as:

$$\hat{S} = I_{sc} - \hat{G} \quad (17)$$

Then, the streak interference removal image I_{SIR} is synthesized as:

$$I_{SIR} = \hat{I}_B + \hat{S} \quad (18)$$

4. Result

To verify the effectiveness of our proposed method, some experiments on several outdoor images with weather streak interference (e.g. rain or snow) are presented in this section. In our experiments, two kinds of streaks are used to test the performance. One kind is rainy image, which is synthesized with streak interference and ground truth manually. The other is images with real snowy interference. The compared algorithms include the MCA-based streak removal (MCASR) method in [11], the layer removal with discriminative dictionary (LRDD) method in [13], the segmentation-based streak removal method (SSRM) with multiple dictionary learning in [12], and our proposed method. The parameters in the compared algorithms are tuned as suggested in literatures. Some parameters of our proposed are set as follows. The patch size 8×8 is used in both *GMM* and local dictionary learning. 30 Gaussian components in *GMM* are utilized here due to the limitation patterns of streak interference. The number of atoms in the local dictionary is set to 256, considering the high computational complexity. Furthermore, the peak signal-to-noise ratio (PSNR) is used to objectively evaluate the streak removal performance for the synthesized rainy image. The results of synthesized rain removal are presented in Figure 2, and the removal results of real snowy are shown in Figure 3. Moreover, the PSNR results for the test synthesized rainy images are depicted in Figure 4.



(a) Rainy Image

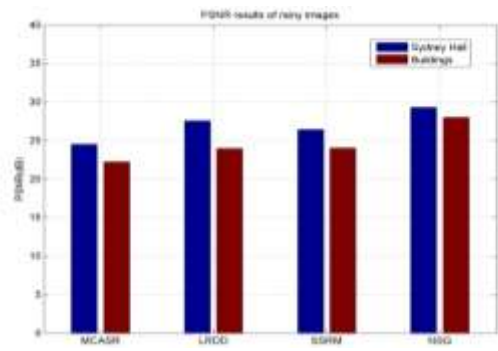
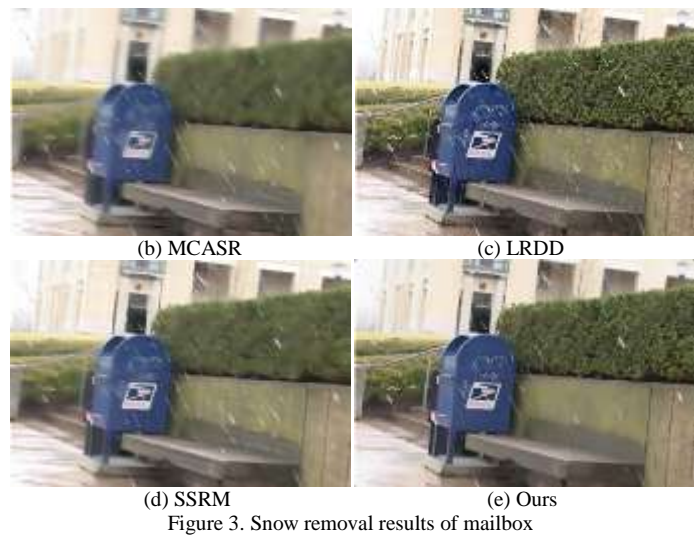
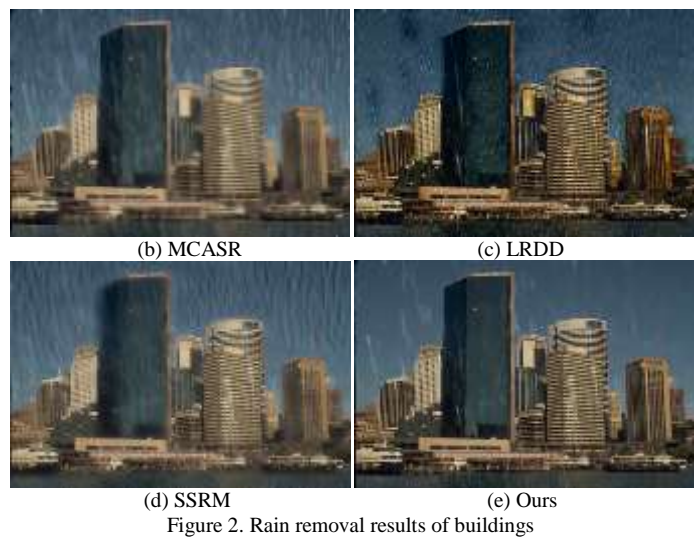


Figure 4. PSNR results of rainy images

5. Conclusion

In this paper, we proposed an approach to solve the problem of weather streak interference removal. Similar to the previous works, we also take the removal task as a layer decomposition problem. The coarse scene background and high-frequency details are firstly separated with the multi-scale analysis tool. Then, different from the previous works, we proposed a joint priors framework to be implemented on the high-frequency component, which learned the dictionary for geometric details and *GMM* for the streak interference layer. Then, an iterative numerical scheme is also developed to solve the objective function in the proposed framework. Some extensive works can be studied on the priors design to better realize the width pattern streak removal such as snow streak in the future.

Acknowledgements

The paper was supported by the National Natural Science Foundation of China (No. 61501147), Natural Science Foundation of Heilongjiang Province (CN) (No. F2015040), China Postdoctoral Science Foundation (No. 2016M601438), and Postdoctoral Science Foundation of Heilongjiang Province (CN) (No. LBH-Z15099).

References

1. O. Ludwig, D. Delgado, V. Goncalves, and U. Nunes, "Trainable Classifiers-Fusion Schemes: An Application to Pedestrian Detection," in *Proceedings of the 12th International IEEE Conference on Intelligent Transportation Systems*, St. Louis, MO, pp. 1-6, 2009
2. M. S. Shehata, J. Cai, W. M. Badawy, T. W. Burr, M. S. Pervez, R. J. Johannesson, et al., "Radmanesh, Video-based Automatic Incident Detection for Smart Roads: The Outdoor Environmental Challenges Regarding False Alarms," *IEEE Transactions on Intelligent Transportation Systems*, No. 9, pp. 349-360, 2008
3. L. Itti, C. Koch, and E. Niebur, "A Model of Saliency-based Visual Attention for Rapid Scene Analysis," *IEEE Transactions on Pattern Analysis and Machine Intelligence*, No. 20, pp. 1254-1259, 1998
4. S. Liu, X. Cheng, W. Fu, Y. P. Zhou, and Q. Z. Li, "Numeric Characteristics of Generalized M Set with its Asymptote," *Applied Mathematics and Computation*, Vol. 243, pp. 767-774, 2014
5. S. Liu, W. Fu, L. He, J. T. Zhou, and M. Ma, "Distribution of Primary Additional Errors in Fractal Encoding Method," *Multimedia Tools and Applications*, No. 76, No. 4, pp. 5787-5802, 2017
6. U. Z. Pan, W. Fu, and X. Cheng, "Fractal Generation Method based on Asymptote Family of Generalized Mandelbrot Set and its Application," *Journal of Nonlinear Science and Applications*, No. 10, pp. 1148-1161, 2017
7. K. Garg and S. K. Nayar, "Detection and Removal of Rain from Videos," in *Proceedings of the 2004 IEEE Computer Society Conference on Computer Vision and Pattern Recognition*, pp. 528-535, 2004
8. X. Zhang, H. Li, Y. Qi, W. K. Leow, and T. K. Ng, "Rain Removal in Video by Combining Temporal and Chromatic Properties," in *Proceedings of IEEE International Conference on Multimedia and Expo*, Toronto, ON, Canada, pp. 461-464, July 2006
9. P. C. Barnum, S. Narasimhan, and T. Kanade, "Analysis of Rain and Snow in Frequency Space," *International Journal of Computer Vision*, No. 86, pp. 256-274, January 2010
10. J. Bossu, N. Hautière, and J. P. Tarel, "Rain or Snow Detection in Image Sequences Through Use of a Histogram of Orientation of Streaks," *International Journal of Computer Vision*, No. 93, pp. 348-367, 2011
11. L. W. Kang, C. W. Lin, and Y. H. Fu, "Automatic Single-Image-based Rain Streaks Removal via Image Decomposition," *IEEE Transactions on Image Processing*, No. 21, pp. 1742-1755, 2012
12. D. A. Huang, L. W. Kang, M. C. Yang, C. W. Lin, and Y. C. F. Wang, "Context-Aware Single Image Rain Removal," in *Proceedings of IEEE Conference on Multimedia and Expo*, pp. 164-169, 2012
13. Y. Luo, Y. Xu, and H. Ji, "Removing Rain from a Single Image via Discriminative Sparse Coding," in *Proceedings of IEEE International Conference on Computer Vision*, pp. 3399-3405, 2015
14. Y. L. Chen and C. T. Hsu, "A Generalized Low-Rank Appearance Model for Spatio-Temporally Correlated Rain Streaks," in *Proceedings of IEEE International Conference on Computer Vision*, pp. 1968-1975, 2013
15. Y. L. Robby, T. Tan, X. J. Guo, J. Lu, and M. S. Brown, "Rain Streak Removal Using Layer Priors," in *Proceedings of IEEE Conference on Computer Vision and Pattern Recognition*, pp. 2736-2744, 2016
16. N. Eslahi and A. Aghagolzadeh, "Compressive Sensing Image Restoration Using Adaptive Curvelet Thresholding and Nonlocal Sparse Regularization," *IEEE Transactions on Image Processing*, No. 25, pp. 3126-3140, 2016
17. K. P. Upla, M. V. Joshi, and P. P. Gajjar, "An Edge Preserving Multiresolution Fusion: Use of Contourlet Transform and MRF Prior," *IEEE Transactions on Geoscience and Remote Sensing*, No. 53, pp. 3210-3220, 2015
18. A. L. Cunha, J. Zhou, and M. N. Do, "The Nonsampled Contourlet Transform: Theory, Design, and Applications," *IEEE Transactions on Image Processing*, No. 15, pp. 3089-3101, 2006
19. M. Aharon, M. Elad, and A. M. Bruckstein, "The K-SVD: An Algorithm for Designing of Overcomplete Dictionaries for Sparse Representation," *IEEE Transactions on Signal Processing*, No. 54, pp. 4311-4322, 2006
20. D. Zoran and Y. Weiss, "From Learning Models of Natural Image Patches to Whole Image Restoration," in *Proceedings of IEEE International Conference on Computer Vision*, pp. 479-486, 2011
21. J. A. Tropp and A. C. Gilbert, "Signal Recovery from Random Measurements via Orthogonal Matching Pursuit," *IEEE Transactions on Information Theory*, No. 53, pp. 4655-4666, 2007